MOJITO - DECARBONIZED LIME PRODUCTION THROUGH ENHANCED JOINT DIELECTRIC HEATING AND WASTE CARBONACEOUS MATERIAL ADDITION

HORIZON-EIC-2024-PATHFINDERCHALLENGES-01-02 - GRANT AGREEMENT NUMBER: 101221957

Deliverable D4.1:

Report on first principles

Dissemination Level		
PU	Public	*x*
SEN	Sensitive, limited under the conditions of the Grant Agreement	

Document Type		
R	Document, report (excluding the periodic and final reports)	*x*
DEM	Demonstrator, pilot, prototype, plan designs	
DEC	Websites, patents filing, press & media actions, videos, etc.	
DATA	Data sets, microdata, etc.	
DMP	Data management plan	
ETHICS	Deliverables related to ethics issues.	
SECURITY	Deliverables related to security issues	
OTHER	Software, technical diagram, algorithms, models, etc.	

Due Date: *31/03/2026* (Month 6)
Submission date: *30/03/2026*
Reference Period: *1/10/2025 – 30/9/2028*
Deliverable Lead Partner: *UNIBO*

Disclaimer: Funded by the European Union under Grant #101221957. Views and opinions expressed are however those of the author(s) only and do not necessarily reflect those of the European Union or CINEA. Neither the European Union nor the granting authority can be held responsible for them.

General Information

GA Number: 101221957
Start date of project: 01/10/2025
Project Duration: 3 years
Project website: https://www.mojito-project.eu/

MOJITO consortium

Short	Beneficiary	Role
UNIBO	Alma Mater Studiorum – Università di Bologna	CO
FRA	Fraunhofer UMSICHT	BEN

CO…Coordinator, BEN…Beneficiary, AP…Associated Partner

FOR INTERNAL DOCUMENTATION PURPOSES					
REV.	**DATE**	**DESCRIPTION**	**PAGES**	**CHECKED**	**APPROVED**
1	18/03/2026	First Draft	13		
2	27/03/2026	Final version	12		

Table of Contents

EXECUTIVE SUMMARY 4
1. INTRODUCTION 4
2. COMPUTATIONAL METHODOLOGY 5
3. REACTION ENERGETICS FOR CO2 REMOVAL IN CACO3 POLYMORPHS 5
4. ACTIVATION BARRIERS AND REACTION PATHS ON SELECTED CALCITE SURFACES 7
5. ATOMISTIC INTERPRETATION OF THE CALCINATION PROCESS 10
CONCLUSIONS 11
REFERENCES 12

Executive Summary

This deliverable reports the first-principles investigation of the calcination process carried out in Task 4.1 during project months M1-M6. The work focused on the atomistic description of CO_2 removal from $CaCO_3$ systems, with the aim of clarifying the energetic cost of the process and the main features of the associated reaction pathways. The analysis was performed within a density functional theory framework and considered the three main $CaCO_3$ polymorphs, namely calcite, aragonite, and vaterite, through both bulk and surface models.

The results show that calcite is the most relevant $CaCO_3$ polymorph under the operating conditions considered in this work, whereas aragonite and vaterite are stabilised under different pressure regimes. Under the DFT conditions adopted, the elementary CO_2 removal step is associated with a significant energetic cost in all investigated cases. At the same time, the calculations indicate that both reaction energetics and activation barriers are strongly influenced by the local chemical and structural environment. In particular, the analysis of selected calcite surface models shows that undercoordinated environments represented by stepped surfaces provide a more favourable pathway for CO_2 removal than ideal flat terraces.

The atomistic analysis further indicates that calcination is not a purely rigid bond-breaking event, but involves a coupled structural and electronic reorganisation of the carbonate group and of the surrounding surface environment. These results provide the first mechanistic basis for the interpretation of calcination within MOJITO and establish a reference framework for the subsequent modelling activities planned in the project.

1 Introduction

Calcium oxide (CaO), commonly referred to as lime, is a key material for several industrial sectors, including steelmaking, construction, and engineering applications. It is conventionally produced through the calcination of calcium carbonate ($CaCO_3$), a thermally activated decomposition process that leads to the formation of CaO and CO_2 [1]. Due to the high temperatures required, calcination is associated with significant energy consumption and substantial carbon emissions, making it a relevant target for process intensification and decarbonisation strategies.

The MOJITO project addresses this challenge by exploring alternative process conditions and advanced modelling strategies to improve the efficiency and sustainability of limestone calcination. However, a predictive atomistic description of calcination remains highly challenging. This process is expected to depend strongly on the local structural environment, while the determination of reaction pathways and activation barriers for CO_2 release is computationally demanding. In this context, WP4 aims to elucidate the microscopic mechanisms governing calcination, support the interpretation of experimental observations, and guide experimental activities and subsequent simulations. This effort is essential to establish a robust atomistic picture of calcination and to connect first-principles calculations with larger-scale molecular dynamics simulations.

Deliverable D4.1 addresses the first-principles investigation of the calcination process, in line with Task 4.1. The goal is to characterise the energetics of CO_2 removal from $CaCO_3$ polymorphs and to identify the key features of the associated reaction pathways. The analysis focuses on calcite, aragonite, and vaterite, with particular attention to local atomic environments relevant to experimental systems, including flat and stepped surfaces. Establishing an atomistic description of the reaction energetics is essential to clarify how local structure affects the onset of calcination and to provide a quantitative basis for estimating the timescales that may be accessed by the molecular dynamics simulations planned in Task 4.4.

This deliverable reports the activities carried out in Task 4.1 during project months M1-M6. It summarises the computational framework adopted for the first-principles investigation, the systems and configurations considered, and the main results obtained on calcination energetics and reaction

pathways within the reporting period. In the present deliverable, the term CO_2 removal is used to indicate the elementary atomistic step underlying the calcination process.

2 Computational Methodology

The first-principles calculations reported in this deliverable were performed within the framework of density functional theory (DFT) using the Quantum ESPRESSO package [2]. A spin-polarised formalism was adopted throughout all calculations as a standard choice to consistently account for possible localised electronic states arising during CO_2 removal, particularly in configurations where undercoordinated oxygen atoms may remain in the system. The Perdew-Burke-Ernzerhof (PBE) exchange-correlation functional [3] was used together with projector augmented-wave (PAW) pseudopotentials. Dispersion interactions were included through the Grimme D3 correction [4].

The investigation considered both bulk and surface slab models for the three $CaCO_3$ polymorphs analysed in this work, namely calcite, aragonite, and vaterite. For the slab calculations, the surfaces considered were calcite (104), aragonite (011), and vaterite (010). Periodic boundary conditions were applied in all cases. In the surface models, a vacuum region was introduced along the direction perpendicular to the slab to prevent spurious interactions between periodically repeated images. All atomic coordinates were fully relaxed, with no positional constraints imposed during structural optimisation.

The relative stability of the $CaCO_3$ polymorphs as a function of pressure was assessed through variable-cell relaxation calculations performed under different isotropic external pressures. For each pressure value, the equilibrium structure and the corresponding enthalpy, $H = E + PV$, were evaluated within the same computational framework described above.

The reaction energy E_{react} associated with CO_2 removal was evaluated as

$$E_{react} = E_{fin} + E_{CO_2,iso} - E_{init}$$

where E_{init} is the total energy of the starting bulk or slab model, E_{fin} is the total energy of the corresponding structure after removal of one CO_2 unit, and $E_{CO_2,iso}$ is the energy of an isolated CO_2 molecule computed in a separate simulation cell. This definition was adopted consistently for both bulk and surface models to compare the energetic cost of CO_2 removal across different polymorphs and local atomic environments.

The activation barriers and reaction paths associated with CO_2 removal were investigated using the nudged elastic band (NEB) method [5]. Because the identification of reliable final states is crucial for the atomistic description of dissociation processes, the final configurations adopted in the NEB calculations were first determined using the Xsorb code [6], developed by our group, which was employed to identify the most favourable adsorption geometry of the dissociated final state. A standard NEB optimisation was then performed to obtain a preliminary minimum-energy path between the initial and final states, followed by a climbing-image refinement [7] to achieve a more accurate estimate of the transition state and corresponding activation barrier. This workflow was applied to the selected CO_2 removal processes analysed in the present deliverable.

3 Reaction energetics for CO_2 removal in $CaCO_3$ polymorphs

The first objective of this deliverable is to evaluate the energetic cost associated with CO_2 removal from the three main $CaCO_3$ polymorphs, namely calcite, aragonite, and vaterite, considering bulk models. As a first step, the relative stability of the three bulk polymorphs as a function of pressure was evaluated using the variable-cell relaxation protocol described in Section 2. This analysis was used to determine the pressure conditions under which each polymorph is energetically favoured within the present DFT framework, and thus to establish the most appropriate thermodynamic conditions for comparing their reactivity.

The results are reported in Figure 1. According to the present calculations, vaterite is favoured under tensile stress conditions, i.e., at negative pressures, with an enthalpy crossover with calcite occurring at approximately −3.5 GPa. Calcite is the most stable polymorph in the pressure range closest to ambient conditions, up to about 4.0 GPa, above which aragonite becomes the most stable phase.

These trends are consistent with the well-established picture in which calcite is the stable polymorph under ambient conditions [8], aragonite is favoured at higher pressures [9], and vaterite is a metastable and relatively rare phase. While the transition pressures obtained here are quantitatively shifted with respect to experimental values reported in the literature [10], this discrepancy is expected given the zero-temperature DFT framework employed. In particular, the absence of thermal and entropic contributions in the present treatment may lead to a shift in the calculated crossover pressures. Nevertheless, the relative stability sequence of the polymorphs is correctly reproduced.

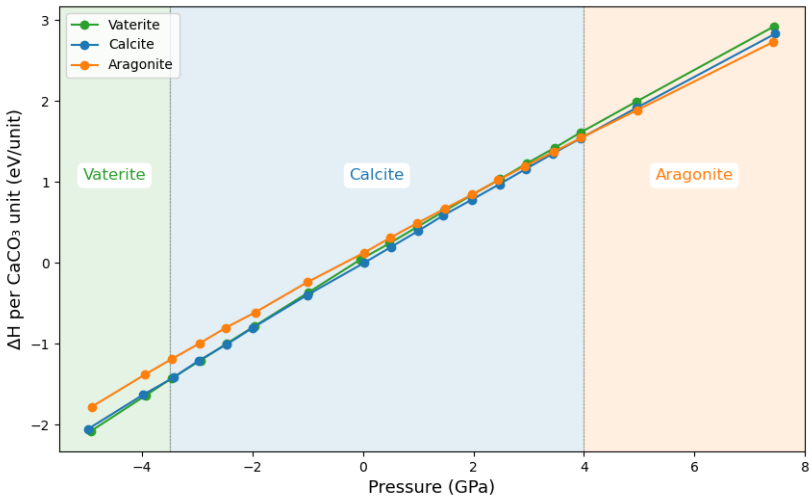

Figure 1. Enthalpy versus pressure curves for the three $CaCO_3$ polymorphs (calcite, aragonite, and vaterite), computed from vc-relax calculations at T = 0 K. The intersections between the curves identify the pressure regions in which each phase is enthalpically favoured within the DFT framework.

Once the relevant stability conditions of the three polymorphs had been identified, we evaluated the energetic cost associated with CO_2 removal from the bulk structures under the corresponding equilibrium pressure conditions, namely from -5.0 to -3.5 GPa for vaterite, from -3.5 to 4 GPa for calcite, and from 4 to 7.5 GPa for aragonite. In each case, one CO_2 unit was removed from a carbonate group in order to mimic a local calcination event in the bulk. The reaction energy E_{react} was then evaluated as explained in Section 2.

Bulk $CaCO_3$ polymorphs	Pressure stability range (GPa)	E_{react} range for CO_2 removal (eV)
Vaterite	$-5.0 \leq P \leq -3.5$	6.07 → 6.01
Calcite	$-3.5 < P < 4.0$	5.80 → 5.54
Aragonite	$4.0 \leq P \leq 7.5$	4.61 → 4.39

Table 1. Calculated E_{react} for CO_2 removal from the bulk structures of $CaCO_3$ polymorphs (vaterite, calcite, and aragonite). The arrows in the E_{react} column indicate the variation of energy across the pressure range; notably, lower pressures correspond to higher energy values.

The calculated energetic costs are reported in Table 1. In all three bulk polymorphs, CO_2 removal is associated with a substantial energetic cost, exceeding 4 eV in every case. Among the investigated structures, aragonite exhibits the lowest value on average (4.50 eV), followed by calcite (5.70 eV),

while vaterite shows the highest cost (6.04 eV). These results indicate that the energetic cost of local CO_2 removal depends sensitively on the structural arrangement of the polymorph.
Subsequently, we evaluated the energetic cost associated with CO_2 removal from the surfaces of the three polymorphs under representative equilibrium pressure conditions. Since the experimental calcination conditions targeted in MOJITO fall within the stability region where calcite is the thermodynamically stable polymorph [11], we focused on pressures within its stability field. Accordingly, we selected pressures corresponding to the phase transitions toward calcite, namely −3.5 GPa for vaterite and 4.0 GPa for aragonite, while for calcite we considered P = 0 GPa, consistent with typical experimental calcination conditions. The most stable surface terminations were adopted for each polymorph: (104) for calcite, (011) for aragonite, and (010) for vaterite [12]. The results reported in Table 2 show that the same qualitative trend already observed for the bulk structures is also found for the surface models. In particular, the energetic cost of CO_2 removal is lowest for aragonite and higher for calcite. In the case of vaterite, however, the tensile conditions required to stabilise this polymorph lead to an unstable slab structure, preventing a reliable evaluation of the CO_2 removal energy at surface level. These results indicate that the relative ease of CO_2 removal remains sensitive to the structural characteristics of the polymorph also at the surface level, although the process remains energetically demanding in all cases successfully investigated.

Surface $CaCO_3$ polymorphs	Pressure (GPa)	E_{react} CO_2 removal (eV)
Calcite (104)	P = 0	5.12
Aragonite (011)	P = 4	4.58

Table 2. Calculated E_{react} for CO_2 removal from the surface structures of $CaCO_3$ polymorphs (calcite (104), and aragonite (011)).

For the purposes of the present deliverable, the subsequent analysis of reaction pathways and activation barriers was focused on calcite-based models, as calcite is the polymorph relevant under the operating conditions of interest for the experimental activities.

4 Activation barriers and reaction paths on selected calcite surfaces

Following the comparative analysis of CO_2 removal energetics in different $CaCO_3$ polymorphs, a more detailed investigation of the reaction pathways and activation barriers was carried out for selected calcite surface models. Calcite was chosen as the reference system for this analysis because it represents the most relevant polymorph under the calcination conditions considered in the experiments. Two distinct local environments were examined, namely a flat surface and a stepped surface, in order to assess how the local coordination of the carbonate group affects the elementary CO_2 removal step. In this context, the stepped surface was adopted as a realistic model of undercoordinated sites that may be found in experimentally relevant systems, including surface defects, grain boundaries, and edge-like environments in nanoclusters or nanoparticles. Previous modelling work on calcite has explicitly considered steps and kinks on the cleavage face, and the literature supports the use of stepped planes as representative models for growth steps on the calcite (104) surface [13-14]. In particular, step edges provide a direct structural analogue of the low-coordination environments characteristic of nanocluster and nanoparticle edges, thereby enabling stepped surfaces to effectively mimic these nanoscale edge sites. The combined use of flat and stepped surfaces also allows one to sample a broader range of local coordination environments than ideal terraces alone, while retaining a clear connection with experimentally relevant calcite particles of micrometre-scale dimensions [15]. The structural models of the flat and stepped surfaces of calcite (104) employed in this work are shown in Figure 2.

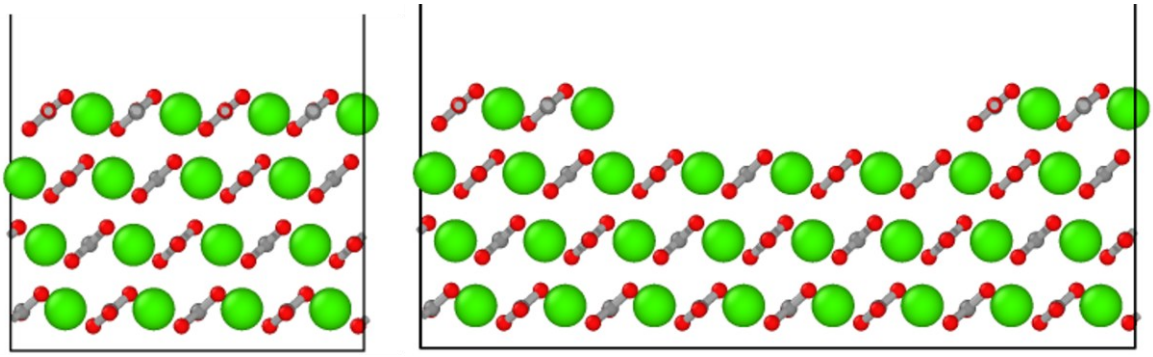

(a) flat surface calcite (104) (b) stepped surface calcite (104)

Figure 2. Structural models of the calcite (104) surface considered in this work: (a) flat surface and (b) stepped surface.

The comparison between flat and stepped calcite surfaces also allows the exploration of a wider range of local coordination environments than those accessible on an ideal terrace alone. The stepped model is intended to represent a more reactive surface motif, where the carbonate group is more exposed than on the flat surface and therefore may undergo dissociation more easily. In earlier atomistic studies of calcite steps, both acute and obtuse step geometries and the associated kink environments are treated as key structural motifs of the calcite (104) surface, which makes them a suitable reference for modelling undercoordinated reactive sites. At the same time, the literature is not fully uniform on the relative stability of all individual step types, so in the present work the stepped model is used primarily as a physically realistic undercoordinated environment rather than as a uniquely most stable surface defect [14, 16].

For both surface models, the reaction path was determined by NEB calculations between the initial adsorbed configuration and a final state in which the detached CO_2 molecule is adsorbed at the most favourable site identified for the dissociated configuration using Xsorb. For the flat calcite surface, the reaction pathway for CO_2 removal is shown in Figure 3 with the associated activation barrier of 3.14 eV. The corresponding reaction profile is relatively simple, with a single maximum associated with the transition state, followed by a slight decrease in energy as the detached CO_2 molecule relaxes toward the most favourable adsorption site. This behaviour is consistent with an elementary one-step dissociation event in which the main energetic cost is associated with the rupture and rearrangement of the local ionic framework surrounding the departing carbonate unit.

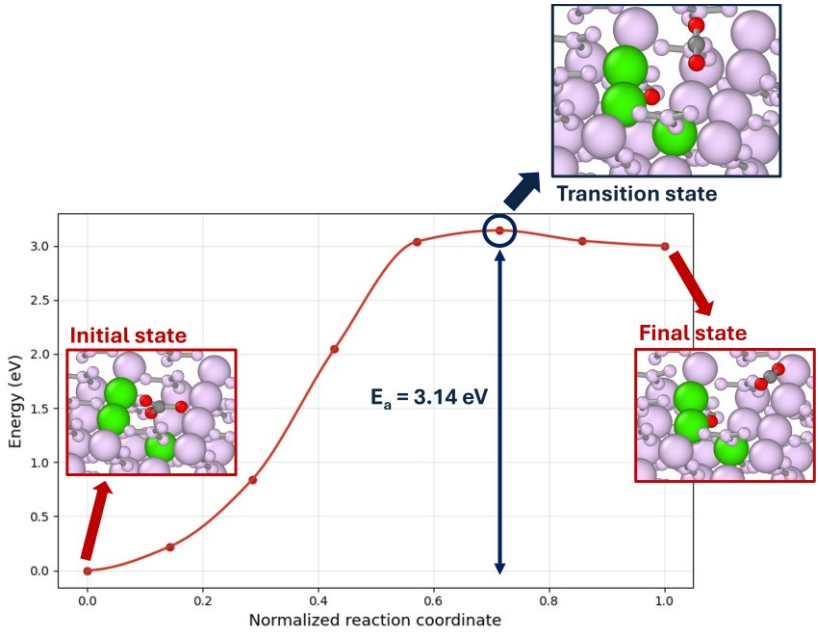

Figure 3. Minimum-energy pathway obtained from NEB calculations for CO_2 removal on the flat $CaCO_3$ (104) surface, together with the corresponding activation energy. The insets display the initial, transition, and final states of the dissociation process.

For the stepped calcite surface, the reaction profile shown in Figure 4 is slightly more complex than that obtained for the flat surface, reflecting the higher structural complexity of the substrate. In particular, the NEB pathway exhibits a few shallow local minima close to the initial state, likely associated with the greater configurational flexibility of the stepped environment, especially upon rearrangement of the carbonate ions. Nevertheless, the overall profile is still characterised by a single main transition-state maximum, followed by a slight energetic stabilisation of the final adsorbed CO_2 configuration. The activation barrier currently obtained for this surface is 2.25 eV. This result already indicates a substantially lower barrier than that found for the flat surface, suggesting that undercoordinated surface environments can facilitate CO_2 removal significantly.

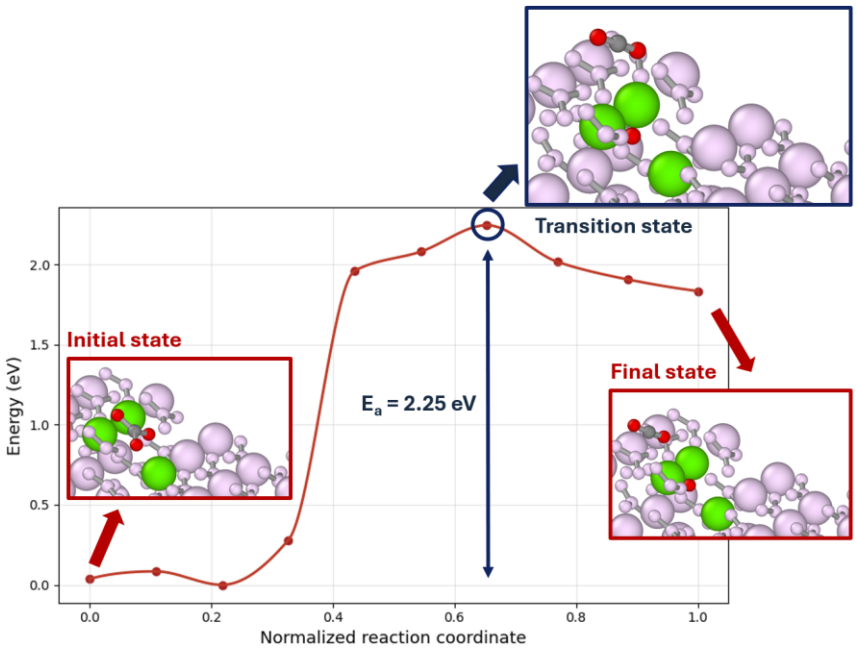

Figure 4. Minimum-energy pathway obtained from NEB calculations for CO_2 removal on the stepped $CaCO_3$ (104) surface, together with the corresponding activation energy. The insets display the initial, transition, and final states of the dissociation process.

This difference can be rationalised in terms of the local atomic structure of the two surface models. On the flat surface, the carbonate group remains more strongly embedded in the ionic surface framework, so that CO_2 removal requires a more extensive rearrangement of the surrounding coordination environment. By contrast, on the stepped surface the carbonate unit is more exposed and less constrained by neighbouring calcium atoms. Therefore, fewer ionic interactions need to be disrupted and rebalanced during dissociation, which is consistent with the lower activation barrier predicted for this model. In this respect, the stepped surface provides a useful atomistic representation of reactive undercoordinated sites, such as edges and locally distorted high-temperature environments, where the elementary step underlying calcination may occur more readily than on ideal flat terraces. This interpretation is also consistent with previous atomistic studies showing that dissolution and detachment processes at calcite steps are strongly sensitive to local step geometry and coordination [16].

Beyond the barrier height itself, the calculated reaction paths also indicate that CO_2 removal is accompanied by a local reorientation of the carbonate group prior to detachment. Interestingly, this feature is consistent with previous first-principles descriptions of $CaCO_3$ calcination reported in the literature. In particular, rotation of the carbonate group prior to CO_2 release has been identified as a key feature of the decomposition pathway leading to CaO formation from $CaCO_3$ structures [17].

Overall, these results show that the activation barrier for CO_2 removal is strongly dependent on the local surface environment. While flat terraces provide a useful reference model, undercoordinated sites represented by stepped surfaces appear to offer a more favourable pathway for the elementary reaction step. This conclusion is particularly relevant for realistic calcite-based systems, where structural heterogeneity is expected to play an important role in determining the onset of calcination. A more detailed atomistic interpretation of the dissociation mechanism is presented in Section 5.

5 Atomistic interpretation of the calcination process

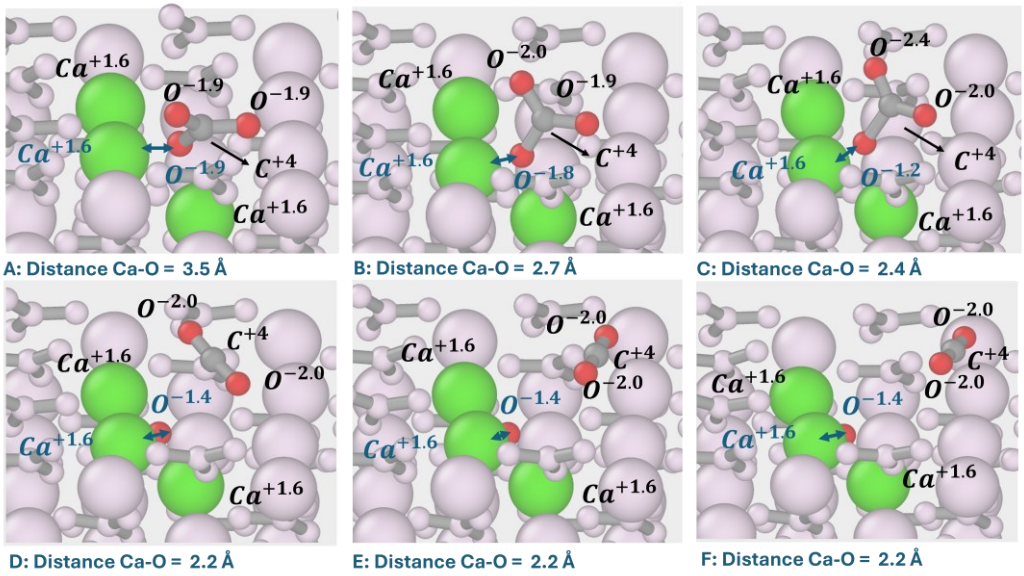

Figure 5. Representative snapshots along the NEB path reported in Figure 3, with the corresponding Bader charges of the carbonate group involved in CO_2 removal and of the neighbouring Ca atoms. Blue labels indicate the distance between a Ca atom and the O atom of the highlighted carbonate group. Carbon, oxygen, and calcium atoms are shown in dark grey, red, and green, respectively, while lighter colours denote atoms not directly involved in the dissociation process.

The results presented in the previous sections show that calcite is the most relevant $CaCO_3$ polymorph under the operating conditions considered in this work, and that CO_2 removal is strongly influenced by the local coordination environment. Calcination should therefore be interpreted as a local atomistic process rather than as a uniform event occurring equivalently at all sites.

At the microscopic level, the calculated pathways show that CO_2 removal is not a purely rigid bond-breaking event. Instead, dissociation is preceded by a local structural rearrangement of the carbonate group. As illustrated in Figure 5, which reports representative configurations along the NEB reaction coordinate, the carbonate unit progressively rotates and exposes the atoms that will form the departing CO_2 molecule, in agreement with previous first-principles descriptions of calcination pathways on calcite surfaces [17]. At the same time, the oxygen atom that remains bound to the surface moves towards the neighbouring calcium atoms, leading to a more favourable coordination of the residual oxide-like species. This behaviour supports a picture in which calcination proceeds through a concerted reorganisation of the local carbonate environment prior to detachment.

Further insight into this mechanism is provided by the analysis of Bader charges calculated for selected images along the reaction path. The charge analysis indicates that CO_2 removal is accompanied by a progressive redistribution of electronic charge within the dissociating carbonate group. In particular, the oxygen atom remaining in the slab becomes less negatively charged as the reaction proceeds and its interaction with nearby calcium atoms increases. At the same time, the charge distribution over the atoms forming the future CO_2 molecule evolves towards a more neutral molecular configuration, until detachment takes place. Although a detailed charge-by-charge discussion is beyond the scope of the present deliverable, this behaviour supports the interpretation of calcination as a coupled structural and electronic reorganisation rather than as the abrupt removal of a pre-formed molecular unit.

The comparison between flat and stepped calcite surfaces confirms that local coordination is a key factor in controlling the elementary reaction step. The lower activation barrier obtained for the stepped surface indicates that undercoordinated environments provide a more favourable pathway for CO_2 removal than ideal flat terraces. This suggests that the onset of calcination is likely to occur preferentially at structurally heterogeneous sites, where the carbonate group is more exposed and the local ionic framework can reorganise more readily during dissociation.

Overall, the calculations reported in this deliverable support a microscopic picture in which calcination is promoted by the combined effect of structural rearrangement and charge redistribution at locally favourable sites. Surface steps, edges, and other undercoordinated environments are therefore expected to play a major role in facilitating CO_2 removal in realistic calcite-based systems. These findings provide a mechanistic basis for the interpretation of calcination at the atomistic level and establish a reference framework for the subsequent modelling activities of the project.

6 Conclusions

This deliverable reports the first-principles investigation of the calcination process carried out in Task 4.1 during project months M1-M6. The work focused on the atomistic description of CO_2 removal from $CaCO_3$ systems through the analysis of phase stability, reaction energetics, and selected reaction pathways and activation barriers.

The results obtained indicate that calcite is the most relevant $CaCO_3$ polymorph under the operating conditions considered in this work, whereas aragonite and vaterite are stabilised under different pressure regimes. Under the DFT conditions considered, the elementary CO_2 removal step remains associated with a significant energetic cost in all the investigated cases. At the same time, the

calculations consistently show that both the reaction energetics and the activation barriers are strongly modulated by the local chemical environment, crystal structure, and surface morphology.

The reaction-path analysis performed on selected calcite surface models further shows that local coordination plays a key role in controlling the elementary dissociation step. In particular, undercoordinated environments represented by stepped surfaces provide a more favourable pathway for CO_2 removal than ideal flat terraces. The atomistic analysis also indicates that the process is not a purely rigid bond-breaking event, but involves a coupled structural and electronic reorganisation, including rotation of the carbonate group, rearrangement of the oxygen atom remaining on the surface, and redistribution of charge during detachment.

Overall, the calculations reported in D4.1 provide a consistent microscopic picture of calcination as a local atomistic process whose energetic accessibility depends strongly on the surrounding structural environment. These results establish the first mechanistic basis for the interpretation of calcination within MOJITO and provide a reference framework for the subsequent modelling activities, including the molecular dynamics simulations planned in the next stage of the project. In this context, structural models of flat and stepped calcite surfaces, together with their interaction with relevant environmental species such as CO_2 and, where appropriate, powdered carbonized materials, will be employed to train machine-learning interatomic potentials within Task 4.3, thereby ensuring an accurate representation of the DFT-derived energetics. The resulting potentials will enable large-scale molecular dynamics simulations in Task 4.4, aimed at exploring the dynamical evolution of the calcination process, assessing the accessibility of CO_2 removal events, and estimating the timescales associated with the process, with validation against the DFT reference data obtained in Task 4.1.

7 References

[1] A. Arizzi, C. Parra-Fernández, Materials and Structures **58**, 152 (2025).
[2] P. Giannozzi, *et al.*, Journal of Chemical Physics **152**, 154105 (2020).
[3] J.P. Perdew, K. Burke, M. Ernzerhof, Physical Review Letters **77**, 3865 (1996).
[4] S. Grimme, J. Antony, S. Ehrlich, H. Krieg, Journal of Chemical Physics **132**, 154104 (2010).
[5] G. Mills, H. Jónsson, G.K. Schenter, Surface Science **324**, 305 (1995).
[6] E. Pedretti, P. Restuccia, M.C. Righi, Computer Physics Communications **291**, 108827 (2023).
[7] G. Henkelman, B.P. Uberuaga, H. Jónsson, Journal of Chemical Physics **113**, 9901 (2000).
[8] Z. Nan, *et al.*, Journal of Colloid and Interface Science, **325**, 331 (2008).
[9] S. Ono, T. Kikegawa, Y. Ohishi, American Mineralogist **92**, 1246 (2007).
[10] X. Zhao, *et al.*, Frontiers in Earth Science **10**, 907967 (2022).
[11] D.P. Hanak, *et al.*, Energy & Environmental Science **8**, 2199 (2015).
[12] Z. Sun, *et al.*, RSC Advances **6**, 39460 (2016).
[13] N.H. de Leeuw, *et al.*, Journal of the Chemical Society, Faraday Transactions **93**, 467 (1997).
[14] R. Kristensen, S.L.S. Stipp, K. Refson, Journal of Chemical Physics **121**, 8511 (2004).
[15] T. Setia Febriatna, P. Setyo Darmanto, F. Bagja Juangsa, Clean Energy **7**, 313 (2023).
[16] N.H. de Leeuw, S.C. Parker, J.H. Harding, Physical Review B **60**, 13792 (1999).
[17] J. Cai, Z. Li, Energy & Fuels **38**, 8145 (2024).